Nonuniversal magnetization at the BEC critical field: Application to the spin dimer compound $Ba_3Mn_2O_8$

S. Suh,[1] K. A. Al-Hassanieh,[2] E. C. Samulon,[3] I. R. Fisher,[3] S. E. Brown,[1] and C. D. Batista[2]

[1]*Department of Physics and Astronomy, University of California, Los Angeles, Los Angeles, California 90095-1547, USA*

[2]*Theory Division, Los Alamos National Laboratory, Los Alamos, New Mexico 87545, USA*

[3]*Geballe Laboratory for Advanced Materials and Department of Applied Physics, Stanford University, Stanford, California 94305, USA*

(Received 7 April 2011; revised manuscript received 13 June 2011; published 5 August 2011)

$Ba_3Mn_2O_8$ is a hexagonally coordinated Mn^{5+} $S = 1$ spin dimer system with small uniaxial single-ion anisotropy. ^{135,137}Ba NMR spectroscopy is used to measure the longitudinal (M_ℓ) magnetization in the vicinity of the critical field at H_{c1} for the onset of magnetic order for $\mathbf{H} \parallel \mathbf{c}$ and $\mathbf{H} \perp \mathbf{c}$. $M_{\ell\parallel}(T, H_{c1})$, $M_{\ell\perp}(T, H_{c1})$ are reproduced by solving a low-energy model for a dilute gas of interacting bosons.

DOI: 10.1103/PhysRevB.84.054413 PACS number(s): 75.10.Jm, 75.40.Cx, 76.60.Cq

Recent investigations of field-induced phases in $S = 1/2$ magnetic insulators typify the opportunities for studying the problem of Bose-Einstein condensates (BECs) specifically,[1] and quantum criticality more generally. In spin-dimer, and other spin-gapped systems, the ground state is a singlet while the lowest energy excited states are triplets.[2,3] The magnetic field tunes the chemical potential for triplets through zero at the critical field H_{c1}, that either condense or crystallize into a superlattice depending on the balance between kinetic and potential energies.[4,5] In some special cases, a coexistence of these two phases is also possible.[6,7] The Hamiltonian has $U(1)$ rotational symmetry for an idealized case, and this symmetry is spontaneously broken in the condensed phase with the development of a finite transverse magnetization M_t.

From what is known about the spin-dimer system $Ba_3Mn_2O_8$,[8] these conditions hold for $\mathbf{H} \parallel \mathbf{c}$,[9] although the evolution of the phases in a magnetic field is known to deviate from the simplest $S = 1/2$ isotropic case in a number of ways.[9–11] Two magnetization plateaus with $\langle S_z \rangle = 1$ (per dimer) and $\langle S_z \rangle = 2$ are a consequence of the $S = 1$ state of the Mn^{5+} ions.[10,12] In addition, a small single-ion uniaxial anisotropy is understood to produce new boundaries in the ordered phases for $\mathbf{H}$ tilted from the $\mathbf{c}$ axis. While this anisotropy is not relevant for $\mathbf{H} \parallel \mathbf{c}$, its influence is evident for $\mathbf{H} \perp \mathbf{c}$, producing an additional phase II stabilized only near $H_{c1\perp}$ and the other critical fields. Further, the hexagonal coordination of the layers leads to geometric frustration. The near-neighbor transverse spin components would be rotated by $\alpha = 120^\circ$ in an isolated triangular layer.[13,14] The stacking of the layers for the trigonal crystal is *abc* (Fig. 1), and interlayer coupling changes the value of α to $\alpha = 120^\circ + \epsilon$ with $\epsilon \sim 9^\circ$ (i.e., it induces an incommensurate spin ordering to partially relieve the interlayer frustration).

Presented here are results of ^{135,137}Ba NMR spectroscopy studies in the high symmetry phase near H_{c1} for orientations $\mathbf{H} \parallel \mathbf{c}$ and $\mathbf{H} \perp \mathbf{c}$. The NMR shifts give the magnetization as a function of temperature at $H = H_{c1}$. The focus here is on the nonuniversal regime, but note that otherwise the results are not inconsistent with the expectations for a BEC quantum critical point (QCP) for $\mathbf{H} \parallel \mathbf{c}$[i.e., $M(T \to 0, H_{c1}) \sim T^{3/2}$]. Both the universal and the nonuniversal ($T > 100$ mK) regimes are well described by using an effective low-energy theory for a dilute gas of bosons, and we expect this result is applicable to other systems. Quantitative differences are observed for $\mathbf{H} \perp \mathbf{c}$, in agreement with the expectation for an Ising-like (Z_2) broken symmetry (phase II). Key to our successful description of the magnetization data is the inclusion of the bare offsite repulsions between triplets, in addition to the hardcore repulsion. As we show below, these contributions to the effective triplet-triplet repulsion are crucial to derive a quantitatively correct low-energy effective theory in the dilute limit. This is an important conclusion that applies to any other quantum magnet in the proximity of a BEC-QCP.

The measurements were performed on a single crystal of $Ba_3Mn_2O_8$ placed inside the mixing chamber of a dilution refrigerator for cooling to $T \geqslant 30$ mK. For reference, the maximum temperature of the ordered phases is $T_m \equiv 0.9$ K.[10] ^{135,137}Ba (^{135,137}I $= 3/2$) NMR spectroscopy was performed in magnetic fields $H \leqslant 120$ kOe using a top-tuned configuration. The platform holding the sample and coil is rotated by an Attocube piezoelectric motor, whereas the crystal orientation was determined by the spectroscopic rotation patterns and verified using Hall sensors. At the higher fields available at the National High Magnetic Field Laboratory (NHMFL), we used a bottom-tuned ^{3}He system. The diagonal hyperfine couplings were determined by comparing high-temperature measurements of the shift ($T \geqslant 20$ K) to susceptibility measurements,[10] with the exception of the Ba(I) site in the $\mathbf{H} \parallel \mathbf{c}$ configuration; for that case, the coupling was inferred from field-induced shifts recorded at $T = 100$ mK. Orbital and quadrupolar couplings were determined from the shifts measured at the lowest temperatures for $H < H_{c1}$, and the site identification was established from the intensity ratio for the Ba(II) site relative to the Ba(I) site (i.e., 2 : 1). χ is modelled by using the mean-field expression[12]

$$\chi = \frac{\chi_0}{1 + \gamma \chi_0}, \tag{1}$$

where χ_0 is the single dimer susceptibility

$$\chi_0 = \frac{2N\beta g^2 \mu_B^2 (1 + 5e^{-4\beta J_0})}{3 + e^{2\beta J_0} + 5e^{-4\beta J_0}}, \tag{2}$$

$\gamma = 3J'/Ng^2\mu_B^2$, $J_0 = 19.0$ K, $J' = J_1 + J_4 + 2(J_2 + J_3) = 7.4$ K, and $g = 1.98$.[9,15] These results appear in Fig. 2, and the relevant NMR parameters are summarized in Table I. In extending the analysis to higher magnetic fields, Eq. (1) is

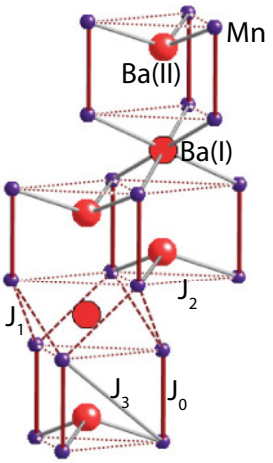

FIG. 1. (Color online) Ionic arrangement of $Ba_3Mn_2O_8$showing location of Ba sites relative to the Mn ions; oxygen ions are not shown. The exchange couplings are indicated by solid (J_0, J_3) and dashed-dotted (J_1, J_2) lines. J_4 is the next-near-neighbor interlayer coupling (not shown).

expected to be valid for $T \geqslant 20$ K in the field range that we used (e.g., 70 kOe, as in Fig. 2).

The established minimal spin Hamiltonian for arbitrarily oriented field direction in $Ba_3Mn_2O_8$ is

$$\mathcal{H} = \sum_{i,j,\mu,\nu} \frac{J_{i\mu jv}}{2} \mathbf{S}_{i\mu} \cdot \mathbf{S}_{jv} + D \sum_{i,\mu} \left(S^z_{i\mu} \cos\theta - S^x_{i\mu} \sin\theta\right)^2 - \mu_B H \sum_{i\mu\alpha\beta} \left(\tilde{g}_{zz} S^z_{i\mu} + \tilde{g}_{xz} S^x_{i\mu}\right), \quad (3)$$

where $\tilde{g}_{zz} = g_{aa} \sin^2\theta + g_{cc} \cos^2\theta$, $\tilde{g}_{xz} = (g_{cc} - g_{aa}) \sin\theta \cos\theta$, $g_{\alpha\beta}$ is the diagonal gyromagnetic tensor with components g_{cc}, $g_{aa} = g_{bb}$, and θ is the angle between the applied field and the c axis. The quantization z axis is set along the field direction. Here i, j designate the dimer coordinates,

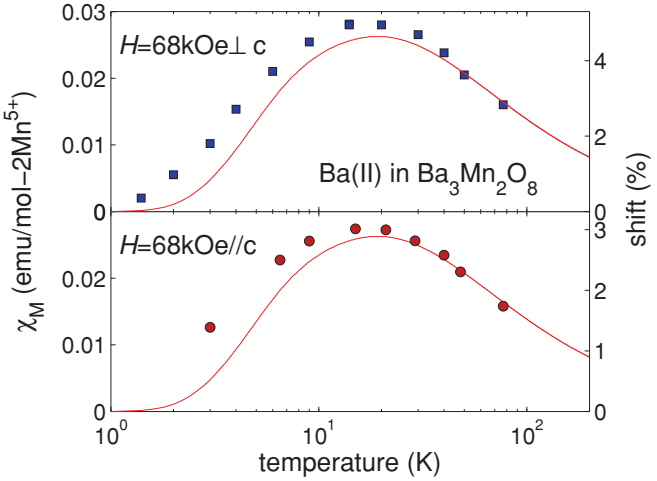

FIG. 2. (Color online) The temperature dependence of the shifts are compared to the dc susceptibility presented in Ref. 12 for the purpose of extracting the diagonal hyperfine couplings for Ba(II) sites. The solid red lines are Eq. (1) (see text), using parameters $J_0 = 19.0$ K, $J' = 7.5$ K.

TABLE I. Diagonal NMR hyperfine coupling parameters and quadrupole frequencies for the Ba(I, II) sites shown in Fig. 1. $\nu_Q \equiv e^2qQ/4$, with $^{135}Q(^{137}Q) = 0.18(0.28) \times 10^{-24}$ cm^2. The hyperfine coupling constants are reported in kG/μ_B-Mn^{5+}.

	A_{aa}	A_{cc}	$^{137}\nu_Q$ (MHz)
Ba(I)	26(1)	35(2)	54.7(2)
Ba(II)	18(1)	11(1)	10.8(2)

$\alpha,\beta = \{x,y,z\}$, $\mu,\nu = \{1,2\}$ denote each of the two $S = 1$ spins in each dimer. The various exchange constants are shown in Fig. 1(a) and are defined as follows: the exchange within a dimer is $J_0 = J_{i,1,i,2}$; the dominant out-of-plane exchange is $J_1 = J_{i,2,j,1}$ for i,j nearest neighbor dimers between planes; the dominant in-plane exchanges between dimers is $J_2 = J_{i,\mu,j,\mu}$ and $J_3 = J_{i,\mu,j,\nu}$ for i,j in plane nearest neighbor dimers and $\mu \neq \nu$; and finally the second largest out-of-plane exchange is $J_4 = J_{i,2,j,1}$ for i,j next nearest neighbor dimers between planes.

Since the dominant exchange interaction is the intradimer coupling J_0, it is more convenient to express $\mathcal{H}$ in a basis that diagonalizes the single dimer Hamiltonian. The single dimer spectrum consists of the singlet ground state, a triplet with energy gap J_0, and a quintuplet of states with energy $3J_0$ relative to the singlet. Since the interdimer exchange is much smaller than J_0 and we are only interested in describing the field region around H_{c1}, to lowest order in perturbation theory, we can eliminate the high-energy quintuplets and restrict $\mathcal{H}$ to the subspace generated by the singlet and the triplets. We note that the energy of the $S^z = 2$ quintuplet at $H = H_{c1}$ is of order J_0 higher than the energy of the singlet and the $S^z = 1$ triplet. Moreover, the $S^z = 2$ quintuplet states are induced by the interdimer exchange terms only when two $S^z = 1$ triplets occupy nearest-neighbor dimers: The pair of triplets is transformed into a singlet and an $S^z = 2$ quintuplet (a pair of quintuplets with opposite values of S^z can be generated from a pair of nearest-neighbor singlets but the energy cost of that process is of order $6J_0$). Therefore, since the density of $S^z = 1$ triplet states is very low near H_{c1}, we can safely neglect the $S^z = 2$ quintuplets in this region of magnetic field.

Based on the previous observations, it is convenient to express the low-energy Hamiltonian in terms of bosonic bond operators that create the singlet ($s_i^\dagger$) and each of the three triplets ($t_{i\uparrow}^\dagger$, $t_{i0}^\dagger$, and $t_{i\downarrow}^\dagger$) on the bond i

$$\begin{aligned} \frac{1}{\sqrt{3}}(|\uparrow\downarrow\rangle_i - |00\rangle_i + |\downarrow\uparrow\rangle_i) &= s_i^\dagger|\emptyset\rangle, \\ \frac{1}{\sqrt{2}}(|\uparrow 0\rangle_i - |0\uparrow\rangle_i) &= t_{i\uparrow}^\dagger|\emptyset\rangle, \\ \frac{1}{\sqrt{2}}(|\uparrow\downarrow\rangle_i - |\downarrow\uparrow\rangle_i) &= t_{i0}^\dagger|\emptyset\rangle, \\ \frac{1}{\sqrt{2}}(|\downarrow 0\rangle_i - |0\downarrow\rangle_i) &= t_{i\downarrow}^\dagger|\emptyset\rangle. \end{aligned} \quad (4)$$

The states $|s^z_{i1}s^z_{i2}\rangle_i$ on the left-hand side are direct products of eigenstates of S^z_{i1} and S^z_{i2}, while s^z_{i1} and s^z_{i2} are the corresponding eigenvalues. $\uparrow$ ($\downarrow$) corresponds to $s_i^z = 1$ ($s_i^z = -1$).

Since the four states on the left-hand side form a basis for the low-energy Hilbert space of the dimer i, the bond operators satisfy the local constraint

$$s_j^\dagger s_j + \sum_\nu t_{j\nu}^\dagger t_{j\nu} = 1, \tag{5}$$

where $\nu = \{\downarrow, 0, \uparrow\}$.

The singlets are condensed for $H \leqslant H_{c1}$. Therefore, the corresponding creation and annihilation operators can be approximated by using the Holstein-Primakoff approximation

$$s_j^\dagger = \sqrt{1 - \sum_\nu t_{j\nu}^\dagger t_{j\nu}}, \tag{6}$$

where we have used the constraint Eq. (5). The spin-wave Hamiltonian is obtained by replacing this expression for $s_j^\dagger$ and s_j in $\mathcal{H}$ and keeping only the terms that are quadratic in the triplet operators. By introducing the triplet operators in momentum space,

$$t_{\mathbf{q}\nu}^\dagger = \frac{1}{N}\sum_j e^{i\mathbf{q}\cdot\mathbf{r}_j} t_{j\nu}^\dagger, \tag{7}$$

where N is the total number of dimers, we obtain the following spin-wave Hamiltonian for $\mathbf{H}$ parallel ($\theta = 0$) or perpendicular to the c axis ($\theta = \pi/2$):

$$\tilde{\mathcal{H}}_{\rm sw} = \sum_{\mathbf{q},\mu,\nu} \epsilon_{\mu\nu}(\mathbf{q}) t_{\mathbf{q}\mu}^\dagger t_{\mathbf{q}\nu}^\dagger + \frac{\gamma_{\mu\nu}(\mathbf{q})}{2}(t_{\mathbf{q}\mu}^\dagger t_{-\mathbf{q}\nu}^\dagger + t_{-\mathbf{q}\nu} t_{\mathbf{q}\mu}), \tag{8}$$

where $\mu, \nu = \{\downarrow, 0, \uparrow\}$, and

$$\begin{aligned}
\epsilon_{\mu\nu}(\mathbf{q}) &= \Big[J_0 + D\big(1 - 3a_\nu^2/2\big)[(\cos\theta)^2 - 1/3] + \frac{4}{3}\mathcal{J}_\mathbf{q} \\
&\quad - g_{\alpha\alpha}\mu_B H a_\nu\Big]\delta_{\mu,\nu} + \frac{D}{2}(\sin\theta)^2\delta_{|\mu-\nu|,2}, \\
\gamma_{\mu\nu}(\mathbf{q}) &= \frac{4}{3}\mathcal{J}_\mathbf{q}\delta_{a_\mu + a_\nu, 0} \\
\mathcal{J}_\mathbf{q} &= 2(J_2 - J_3)\gamma_\mathbf{q}^2 + \frac{J_1}{2}\gamma_\mathbf{q}^1 + \frac{J_4}{2}\gamma_\mathbf{q}^3 \\
\gamma_\mathbf{q}^1 &= \cos q_3 + \cos(q_3 - q_1) + \cos(q_3 - q_2), \\
\gamma_\mathbf{q}^2 &= \cos q_1 + \cos q_2 + \cos(q_1 - q_2), \\
\gamma_\mathbf{q}^3 &= \cos(q_3 - q_2 + q_1) + \cos(q_3 - q_1 + q_2) \\
&\quad + \cos(q_3 - q_1 - q_2).
\end{aligned} \tag{9}$$

Here $\alpha = c$ ($\alpha = a$) for $\mathbf{H}$ parallel (perpendicular) to the c axis, $a_\uparrow = 1$, $a_\downarrow = -1$, and $a_0 = 0$. We note that the expression in Eq. (8) is not valid for intermediate values of θ (i.e., for $0 < \theta < \pi/2$).[16] The diagonal form of $\tilde{\mathcal{H}}_{\rm sw}$,

$$\mathcal{H}_{\rm sw} = \sum_{\mathbf{q}\mu}\left[\omega_{\mathbf{q}\mu}\left(b_{\mathbf{q}\mu}^\dagger b_{\mathbf{q}\mu} + \frac{1}{2}\right) - \frac{\epsilon_{\mu\mu}}{2}\right], \tag{10}$$

is obtained by means of a standard Bogoliubov transformation. The z component of the magnetization is a good quantum number for $\theta = 0$ because $\mathcal{H}$ is invariant under a uniform spin rotation along the z axis. Therefore, the three branches of Bogoliubov quasiparticles have the same label $\nu = \{\uparrow, 0, \downarrow\}$ of the triplet bond operators. In this case, the three dispersion relations are given by

$$\omega_{\mathbf{q}\nu}^0 = \sqrt{\Delta_\nu^2 + \tfrac{8}{3}\Delta_\nu \mathcal{J}(\mathbf{q})} + g_{cc}\mu_B H a_\nu, \tag{11}$$

where $\Delta_\nu = J_0 + \frac{2D}{3} - D a_\nu^2$. Equation (11) shows that the $\nu = 0$ branch does not change in presence of the field, while the full $\nu = \uparrow$ ($\nu = \downarrow$) branch increases (decreases) linearly in field without changing its shape. This is a direct consequence of the invariance of $\mathcal{H}$ under a uniform spin rotation along the z axis. The low-temperature properties close to H_{c1} are determined by the lowest energy branch $\nu = \uparrow$ that becomes gapless at the critical point

$$H_{c1}(\theta = 0) = \sqrt{\left(J_0 - \frac{D}{3}\right)^2 + \frac{8}{3}\left(J_0 - \frac{D}{3}\right)\mathcal{J}(\mathbf{Q})}/g_{cc}\mu_B.$$

$\mathbf{Q} = (\alpha_m, -\alpha_m, 0)$ is the wave vector that minimizes $\omega_{\mathbf{q}\uparrow}^0$ with α_m determined by

$$\cos\alpha_m = \frac{J_1 - 2(J_2 - J_3)}{4(J_2 - J_3 - J_4)}. \tag{12}$$

Since the shape of $\omega_{\mathbf{q}\nu}^0$ does not change with field, $\omega_{\mathbf{q}\uparrow}^0$ increases quadratically in $|\mathbf{q} - \mathbf{Q}|$.

The situation is qualitatively different for $\theta = \pi/2$ because the magnetization along the field axis is no longer conserved. The continuous $U(1)$ symmetry group of rotations around the z axis is replaced by a Z_2 symmetry. Consequently, the field-induced critical point is Ising-like instead of the BEC-QCP obtained for $\theta = 0$. Another consequence of this reduction in the symmetry of $\mathcal{H}$ is that the index ν of the Bogoliubov quasiparticles does not correspond to a well defined magnetization. To write down the dispersion relations associated with the three branches of Bogoliubov quasiparticles, it is convenient to introduce the following functions:

$$\begin{aligned}
F_\mathbf{q} &= \epsilon_{\uparrow\uparrow}^2(\mathbf{q}) + \epsilon_{\downarrow\downarrow}^2(\mathbf{q}) + 2\big(D^2/4 - 16\mathcal{J}_\mathbf{q}^2/9\big) \\
G_\mathbf{q} &= [\epsilon_{\uparrow\uparrow}^2(\mathbf{q}) - \epsilon_{\downarrow\downarrow}^2(\mathbf{q})]^2/4 \\
&\quad - 2\epsilon_{\uparrow\uparrow}(\mathbf{q})\epsilon_{\downarrow\downarrow}(\mathbf{q})\big(D^2/4 + 16\mathcal{J}_\mathbf{q}^2/9\big) \\
&\quad + [\epsilon_{\uparrow\uparrow}^2(\mathbf{q}) + \epsilon_{\downarrow\downarrow}^2(\mathbf{q})]\big(D^2/4 - 16\mathcal{J}_\mathbf{q}^2/9\big),
\end{aligned} \tag{13}$$

where the functions $\epsilon_{\mu\nu}(\mathbf{q})$ are evaluated at $\theta = \pi/2$. The resulting expressions for the three dispersion relations are

$$\begin{aligned}
\omega_{\mathbf{q}\uparrow}^{\pi/2} &= \sqrt{F_\mathbf{q} - \sqrt{G_\mathbf{q}}} \\
\omega_{\mathbf{q}0}^{\pi/2} &= \sqrt{\epsilon_{00}^2(\mathbf{q}) - 16\mathcal{J}_\mathbf{q}^2/9} \\
\omega_{\mathbf{q}\downarrow}^{\pi/2} &= \sqrt{F_q + \sqrt{G_q}}.[3pt]
\end{aligned} \tag{14}$$

The lowest energy branch, $\omega_{\mathbf{q}\uparrow}^{\pi/2}$, becomes gapless at the critical field

$$\begin{aligned}
[g_{aa}\mu_B H_{c1}(\theta = \pi/2)]^2 &= \left(J_0 + \frac{D}{6}\right)^2 + \frac{8}{3}\left(J_0 + \frac{D}{6}\right)\mathcal{J}(\mathbf{Q}) \\
&\quad - \frac{D^2}{4} - \frac{4}{3}|D||\mathcal{J}(\mathbf{Q})|.
\end{aligned} \tag{15}$$

The minimum is still at $\mathbf{q} = \mathbf{Q}$ but, in contrast to the $\theta = 0$ case, $\omega^{\pi/2}_{\mathbf{q}\uparrow}$ increases linearly in $|\mathbf{q} - \mathbf{Q}|$ for $H = H_{c1}$. This is the expected behavior for an Ising-like quantum critical point (the dynamical exponent is $z = 1$).

To compute the low-temperature properties close to H_{c1} we will only keep the lowest energy branch $\omega^{\eta}_{\mathbf{q}\uparrow}$ ($\eta = 0, \pi/2$) of bosonic quasiparticles. Therefore, close to H_{c1} the problem is reduced to a dilute gas of interacting bosons with dispersion relation $\omega^{\eta}_{\mathbf{q}\uparrow}$. Since $g_{\alpha\alpha}\mu_B H_{c1}$ is much bigger than any of the interdimer exchange couplings, the Bogoliubov quasiparticles do not differ significantly from the triplet bond operators. Therefore, we will approximate the interaction between Bogoliubov quasiparticles by the interaction between triplets. The triplet particles $t^{\dagger}_{j\uparrow}$ are hardcore bosons that in addition have an offsite repulsion produced by the Ising component of the interdimer exchange. The exchange constants[15] and the g factors are $J_1 = 0.118$ meV, $J_2 - J_3 = 0.114$ meV, $J_4 = 0.037$ meV, $g_{cc} = 1.98$, and $g_{aa} = 1.97$. The effective repulsive interaction $v_0 = \Gamma_{\mathbf{0}}(\mathbf{Q},\mathbf{Q})$ results for summing the ladder diagrams for the bare interaction vertex[17] $V_{\mathbf{q}}$

$$\Gamma_{\mathbf{q}}(\mathbf{k},\mathbf{k}') = V_{\mathbf{q}} - \int_{-\pi}^{\pi} \frac{d^3p}{8\pi^3} V_{\mathbf{q}-\mathbf{p}} \frac{\Gamma_{\mathbf{p}}(\mathbf{k},\mathbf{k}')}{\omega^0_{\mathbf{k}+\mathbf{p}} + \omega^0_{\mathbf{k}'-\mathbf{p}}} \qquad (16)$$

For $Ba_3Mn_2O_8$, we have $V_{\mathbf{q}} = U + (J_2 + J_3)\gamma^2_{\mathbf{q}} + \frac{J1}{2}\gamma^1_{\mathbf{q}} + \frac{J4}{2}\gamma^3_{\mathbf{q}}$, where $U \to \infty$ comes from the hardcore repulsion, while the rest of the terms correspond to the offsite repulsive interactions. By solving Eq. (16), we obtain $v_0 = 0.9$ meV for $J_2 + J_3 = 2.82$ K, obtained by fitting $H_{c2} \simeq 27$ T for $\mathbf{H} \parallel \mathbf{c}$.

The longitudinal magnetization for $\mathbf{H} \parallel \mathbf{c}$ is shown in Fig. 3(a) for several fields near H_{c1}. The curve measured at $H = H_{c1} = 89.3$ kOe is consistent with the expectation $M_{\ell\parallel} \sim T^{3/2}$ for $T \to 0$, even if the range of temperatures is too limited to demonstrate the universal exponent. The red line is the result of a Hartree-Fock decoupling of the interacting v_0 term whose only effect in the disordered phase is a renormalization of the chemical potential $\mu_{\text{eff}} = \mu - 2v_0\rho$ (ρ is the density of bosons).[2] Calculations for field values differing from H_{c1}, $H = H_{c1} - 1.3$ kOe (blue) and $H = H_{c1} + 1.5$ kOe (green), also match the NMR shift data well. We note that there is a 20% disagreement if only the hardcore repulsion is included in Eq. (16).

When the applied field is rotated to the a-b plane, the ordered phase II bordering the paramagnet is believed to be Ising-like, with transverse spins confined to the **c** direction. The measured magnetization shown in Fig. 3(b) is also in very good agreement with the magnetization curve obtained from the dilute gas approach. The anisotropy term also has the effect of lowering the critical field H_{c1}. In confining the transverse spins to the **c** axis, the energy gain associated with the broken symmetry is reduced slightly, and consequently $M_{\ell\perp} < M_{\ell\parallel}$. The outcome is consistent with the anisotropy parameter $D = 32$ μeV as established by electron paramagnetic resonance.[18]

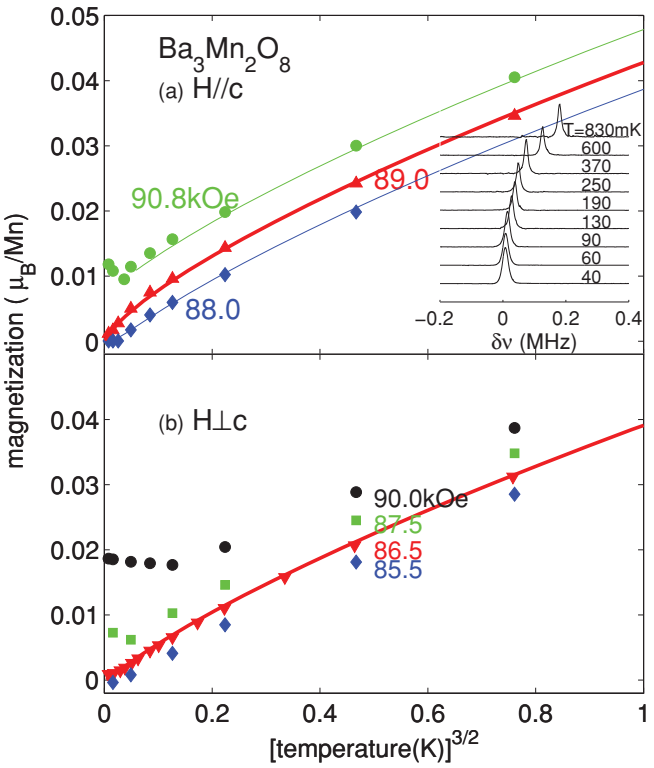

FIG. 3. (Color online) (a) $M_{l\parallel}$ vs T for selected magnetic fields close to $H_{c1\parallel}$. The inset shows a sequence of spectra for the Ba(II) site recorded at different temperatures. The solid curve is from ladder diagram calculations (see text). (b) The same as (a), for $\mathbf{H} \perp \mathbf{c}$.

The ^{135,137}Ba spectroscopy reported here summarizes the behavior near to the critical field at $H = H_{c1}$ for two directions of applied magnetic field. For the longitudinal magnetization, the data is well described by including interdimer (near-neighbor) repulsions in the ladder calculation.

ACKNOWLEDGMENTS

The authors acknowledge helpful discussions with T. Giamarchi, O. Sushkov, and M. Whangbo. This work was supported in part by the NSF under Grants No. DMR-0804625 (SEB), No. DMR-0705087 (IRF), and by the National Nuclear Security Administration of the US Department of Energy at Los Alamos National Laboratory under Contract No. DE-AC52-06NA25396.

[1] T. Giamarchi, C. Rüegg, and O. Tchernyshyov, Nature Phys. **4**, 198 (2008).

[2] T. Nikuni, M. Oshikawa, A. Oosawa, and H. Tanaka, Phys. Rev. Lett. **84**, 5868 (2000).

[3] M. Jaime *et al.*, Phys. Rev. Lett. **93**, 087203 (2004).

[4] K. Kodama, M. Takigawa, M. Horvatic, C. Berthier, H. Kageyama, Y. Ueda, S. Miyahara, F. Becca, and F. Mila, Science **298**, 395 (2002).

[5]T. M. Rice, Science **298**, 760 (2002).
[6]P. Sengupta and C. D. Batista, Phys. Rev. Lett. **98**, 227201 (2007).
[7]P. Sengupta and C. D. Batista, Phys. Rev. Lett. **99**, 217205 (2007).
[8]M. T. Weller and S. J. Skinner, Acta Crystallogr. Sect. C **55**, 154 (1999).
[9]E. C. Samulon, Y.-J. Jo, P. Sengupta, C. D. Batista, M. Jaime, L. Balicas, and I. R. Fisher, Phys. Rev. B **77**, 214441 (2008).
[10]M. Uchida, H. Tanaka, H. Mitamura, F. Ishikawa, and T. Goto, Phys. Rev. B **66**, 054429 (2002).
[11]H. Tsujii, B. Andraka, M. Uchida, H. Tanaka, and Y. Takano, Phys. Rev. B **72**, 214434 (2005).
[12]M. Uchida, H. Tanaka, M. I. Bartashevich, and T. Goto, J. Phys. Soc. Jpn. **70**, 1790 (2001).
[13]R. R. P. Singh and D. A. Huse, Phys. Rev. Lett. **68**, 1766 (1992).
[14]H. Kawamura, J. Phys. Condens. Matter **10**, 4707 (1998).
[15]M. B. Stone, M. D. Lumsden, S. Chang, E. C. Samulon, C. D. Batista, and I. R. Fisher, Phys. Rev. Lett. **100**, 237201 (2008).
[16]E. C. Samulon, K. A. Al Hassanieh, Y.-J. Jo, M. C. Shapiro, L. Balicas, C. D. Batista, and I. R. Fisher, Phys. Rev. B **81**, 104421 (2010).
[17]S. T. Beliaev, Sov. Phys. JETP **7**, 299 (1958).
[18]S. Hill (private communication).